encit 2020

ABCM
Associação Brasileira de Engenharia e Ciências Mecânicas

18th Brazilian Congress of Thermal Sciences and Engineering
November 16-20, 2020 (Online)

ENC-2020-0405
VALIDATION OF THE THEORETICAL MODEL FOR DIMENSIONING THE PROPELLANT CHARACTERISTICS IN A LABORATORY SCALE HYBRID ROCKET MOTOR BENCH

Rodrigo de Melo Silveira
Isabel Pacheco Brasil de Matos
Lia Junqueira Pimont
Paula Cristina Gomes Fernandes
Instituto Tecnológico de Aeronáutica, 12228-900 São José dos Campos, Brazil
silveirarms@ifi.cta.br
isabelbrasildematos@gmail.com
liajpimont@gmail.com
paulacgfernandes7@gmail.com

Leonardo Henrique Gouvêa
Instituto Tecnológico de Aeronáutica, 12228-900 São José dos Campos, Brazil
gouvea@ita.br

Pedro Teixeira Lacava
Instituto Tecnológico de Aeronáutica, 12228-900 São José dos Campos, Brazil
placava@ita.br

Abstract. *Two different hybrid rocket propellant fuels were tested in this work with the purpose of validating a simulation procedure that uses theoretical analysis of the parameters of a pre-existing test bench. Fuels used were high-density polyethylene (HDPE) and hydroxyl-terminated polybutadiene (HTPB) because of their slower burn rate. Validation methodology consists of inputting appropriate propulsion parameters at NASA CEA (Chemical Equilibrium with Applications) tool and at MATLAB® routine and then comparing all obtained parameters from burn simulation with thrust and chamber pressure measured at the test bench using HDPE and HTPB. The same theoretical model was also validated by comparing pre-existing data of Paraffin burns previously made at the same test bench. Results obtained by comparison to all 3 different propellants show that theoretical simulation values are compatible with measured chamber pressure and thrust. Although the proposed model in this work considers a constant regression rate along all the length of the propellant grain, this assumption could be achieved as desired by decreasing effects of a recirculation zone. These results show that a test bench could be reused with any different hybrid propellant, enabling the possibility to study application of new fuel blends. This work can be considered of great value for future studies on hybrid propulsion at a pre-existing test bench.*

Keywords: *Aerospace engineering, hybrid rocket propulsion, propulsion parameters, test bench, hybrid rocket motor.*

1. INTRODUCTION

Although hybrid rocket motors have lower thrust values in comparison to liquid or solid ones (Pastrone, 2012), hybrid rocket propulsion represents a promising alternative for aerospace systems due its low cost and high safety by using inert fuel grain (Karabeyoglu et al., 2011), thus allowing its use in different applications like sounding rockets and low orbit insertion vehicles (Cai et al., 2013a). The theoretical design of hybrid rocket motors is an important first step for the development of laboratory scale benches for this type of motor (Mazzetti et al., 2016).

It is important that due considerations are given to the operating conditions of the bench, so that the expected theoretical values are proven through tests (Cai et al., 2013b). The advantages of preliminary tests on a laboratory scale compared to full-scale tests of rocket motors are the cost reductions (Nagata et al, 2006) and the possibility to study the application of new fuel blends (Kim et al., 2015).

Many papers present the paraffin application as a promising fuel for hybrid propulsion due its high regression rate (Wang et al., 2020). However, it is possible to point out some advantages for other fuels like High Density Polyethylene (HDPE), Hydroxyl Terminated Polybutadiene (HTPB) or fuel blends (Karabeyoglu et al., 2002). The use of HDPE and HTPB in the present work is motivated by the need to evaluate the proposed procedures applied to simulate the regression rate in a slow-burning fuel, allowing a longer burning time. Other motivating factors were also the ease of buying and machining the grain to the geometry needed.

Based on this, the purpose of this work is to validate a simulation procedure that uses theoretical analysis of the parameters of a pre-existing paraffin based test bench at LCPE (*Laboratório de Propulsão, Combustão e Energia*) and then evaluate the applicability of different fuels, like HDPE and HTPB, in this test bench, enabling their use in future studies for experimental characterization of slow-burning fuels for hybrid rocket motors.

2. METHODOLOGY

2.1 Theoretical Model Validation

Since the LCPE test bench was originally designed to operate with paraffin-based propellants (Quadros, 2017), the theoretical analysis proposed in this work will first be applied to simulate paraffin propellant burns in order to validate the present model.

Considering the empirical law for regression rate ($\dot{r}$) in Eq. (1), the first step is to search the literature for applicable values of linear and exponential coefficients, "*a*" and "*n*", respectively. Applicable values are considered the ones measured after the burn of the propellant at a desired range of oxidizer to fuel ratio (O/F) and oxidant mass flux (G_{OX}).

$$\dot{r} = a \, . \, G_{OX}{}^{n} \tag{1}$$

Previous experimental works with paraffin at LCPE test bench (Quadros, 2017) indicate linear and exponential coefficients, respectively, as 0,213 and 0,62. Related range of O/F (1,2-3,2) and G_{OX} (18-41 kg/(m^{2}s)) for paraffin propellant was also presented in this previous study. Fuel mass concentration was 98% paraffin wax, 1,5% carbon black and 0,5% dispersing agent.

Given these 4 initial parameters (*a*, *n*, O/F, G_{OX}), second step is to determine the specific impulse (I_{SP}), the characteristic velocity (C*), and the thrust coefficient (C_F) for each O/F value considered. These calculations were performed with the NASA CEA (Chemical Equilibrium with Applications) tool, that calculates chemical equilibrium product concentrations from any set of reactants, as described in Gordon and Mcbride (1994).

Third and final step of theoretical simulation is to apply all 4 initial parameters as well as 3 NASA CEA parameters (I_{SP}, C*, C_F) to the hybrid rocket motor equations programmed using MATLAB®. As a result, it is possible to obtain values for maximum burning time (t_B), appropriate values for: fuel grain length (L_P) and mass flow rate of oxidizer ($\dot{m}_{OX}$), as well as the variation over time for: chamber pressure ($p_1(t)$), Thrust ($F(t)$), port diameter ($r(t)$), regression rate ($\dot{r}(t)$). Theoretical simulation in this work considers regression rate varying with time, but constant along the length of the propellant grain.

Validation results are presented in section 4.1 of this abstract and show consistency between the main measured parameters from previous experimental works and the results obtained from this proposed theoretical model.

2.2 Theoretical Model Applied to HDPE and HTPB

After the validation step described in section 2.1, experimental tests using HDPE and HTPB were conducted in order to evaluate the applicability of different fuels at LCPE test bench. All three steps previously described are repeated, but prior to these steps, some restrictions related to LCPE test bench limitations shall be considered as presented in Tab. 1.

Table 1. Test Bench limiting parameters.

Parameter	Limit value
Maximum operating chamber pressure (bar)	10
Maximum propellant grain length (mm)	230
Inner diameter of the chamber (mm)	65
Nozzle throat section diameter (mm)	10.4
Nozzle outlet section diameter (mm)	15

For the first step, recent experiments with HDPE (Kim et al., 2015) indicate measured values of coefficients "*a*" and "*n*", respectively, as 0,026 and 0,58, and related range of O/F (4-10) and G_{OX} (36-316 kg/(m^2s)). Experiments with HTPB (Kim et al., 2015) indicate measured values of coefficients "*a*" and "*n*", respectively, as *0,072* and *0,50*, and related range of O/F (2,5-5) and G_{OX} (55-130 kg/(m^2s)).

By completing steps 2 and 3 indicated in section 2.1 and by inputting limiting parameters from Tab. 1 to the hybrid rocket motor equations programmed using MATLAB®, results are theoretical validated values for both HDPE and HTPB (t_B, L_P, $\dot{m}_{OX}$, $p_1(t)$, $F(t)$, $r(t)$, $\dot{r}(t)$). Prior to running MATLAB codes, some interactions, presented in Fig.1., are necessary to make sure these reference values are coherent to the actual burn simulation.

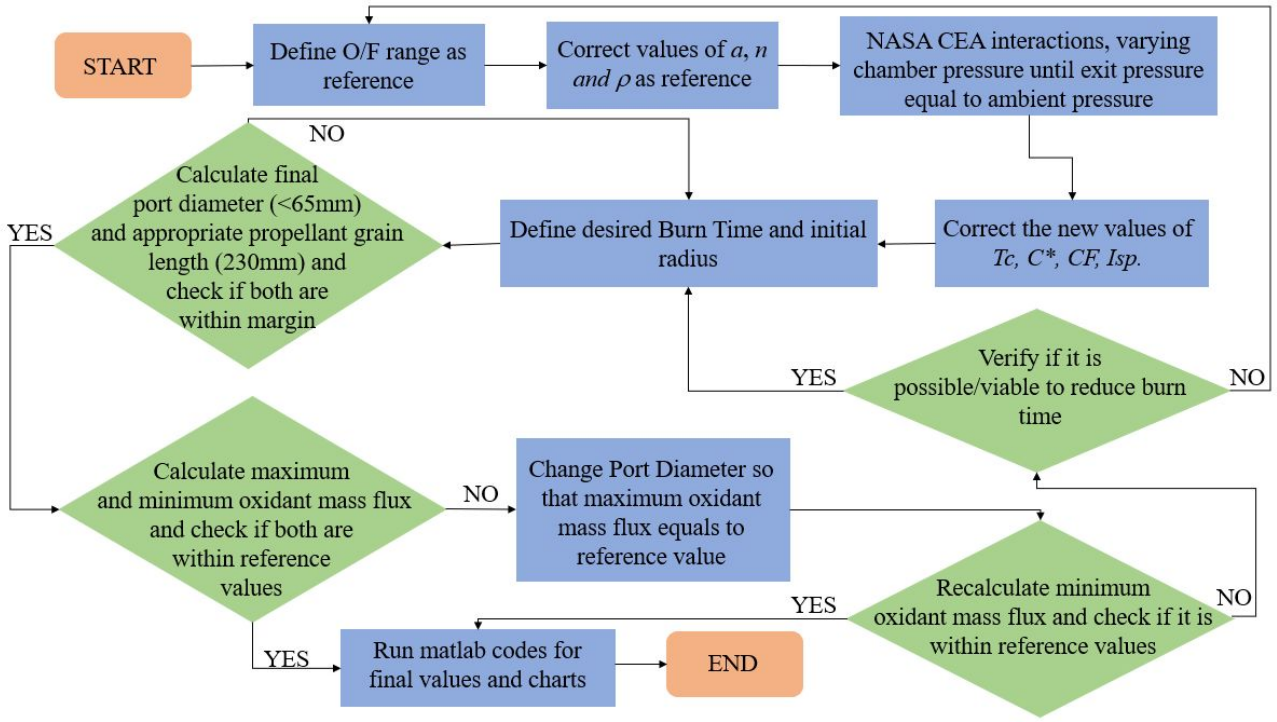

Figure 1. Flowchart explaining how to apply the proposed simulation model.

Comparison results between these validated values and experimental data measured during HDPE and HTPB burns at LCPE test bench are presented in section 4.3 and 4.4.

3. TEST BENCH

The workbench, as shown in Fig. 2, was already applied in previous studies at LCPE and consists of a stainless steel hybrid rocket motor with 65 mm internal diameter and adjustable length between 135 and 265 mm, two cylinders of gaseous oxygen (low and high pressure supply lines) and a cylinder of gaseous nitrogen (used for purging oxygen after burning). All three cylinders are connected to the chamber by means of solenoid valves and a data acquisition system in addition to ignition control and valve opening.

Low pressure supply line is necessary for HDPE and HTPB burns, since the ignitor selected for these propellants needed a manual controlled power source. The ignitor is made by heating a powder mixture of 65% potassium nitrate (KNO_3) and 35% Sorbitol ($C_6H_{14}O_6$) at around 120-130 °C (above the melting point of sorbitol), and casting the mixture into a cylindrical and thin desirable shape. Once cured it forms hard grains which are susceptible to moisture and mechanical impact but can otherwise be stored for several months (Olde et al., 2019). To ignite the system, the ignitor is placed inside the HDPE or HTPB internal diameter, and a nickel-chromium wire is connected to one end of the ignitor, which is then attached to an electrical lead wire to the battery, used as the electrical power source. Paraffin burns previously made at LCPE test bench didn't use this type of igniter and they also didn't need injection of gaseous oxygen at a lower pressure because paraffin needs less activation energy to start its burning process, while HDPE and HTPB ignition takes a longer time (Takashi Nioka et al., 1981).

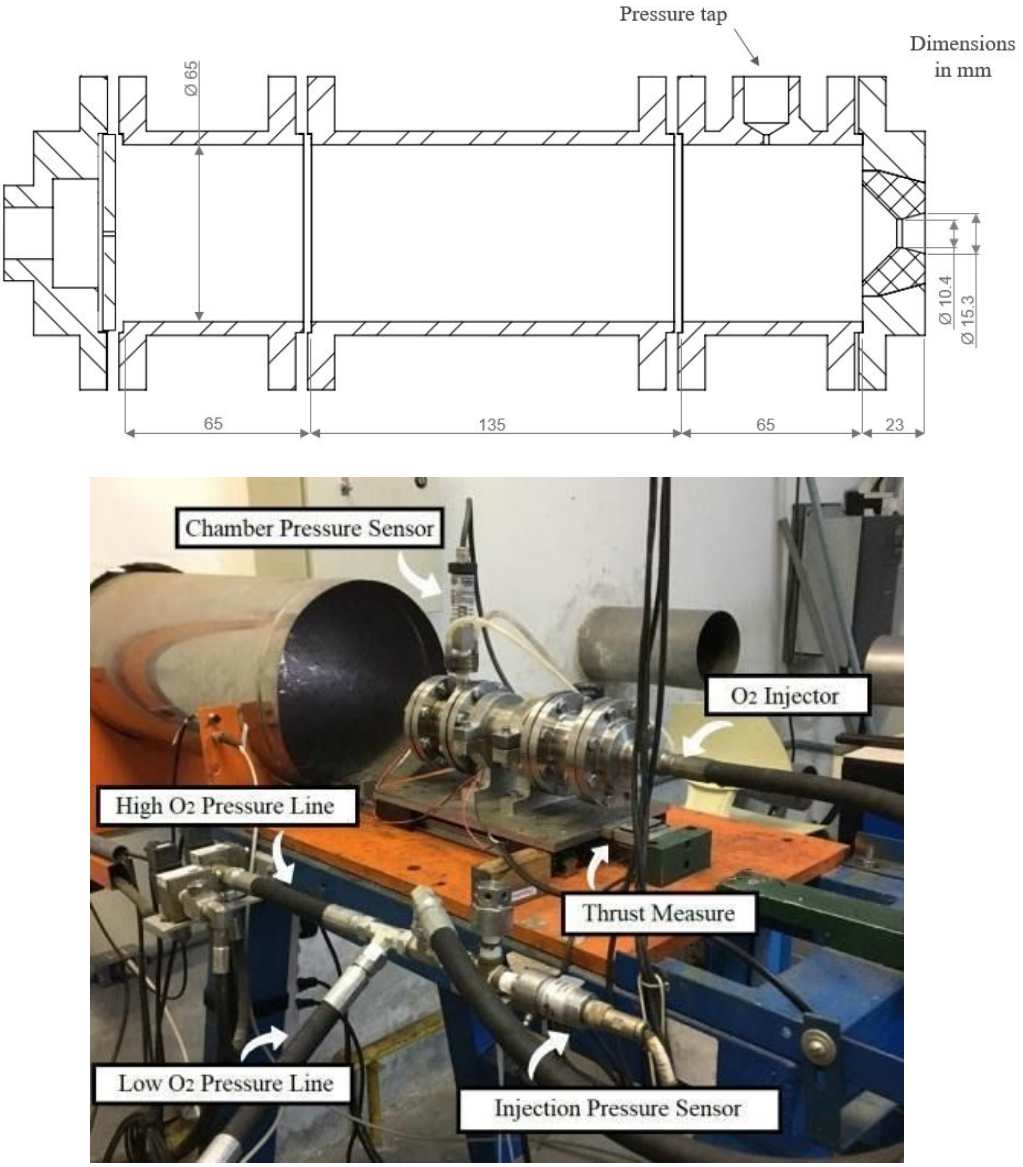

Figure 2. Combustion chamber schematics (upper) and test bench components (bottom).

Logical connections between above mentioned sensors and acquisition board is presented in Fig.3.

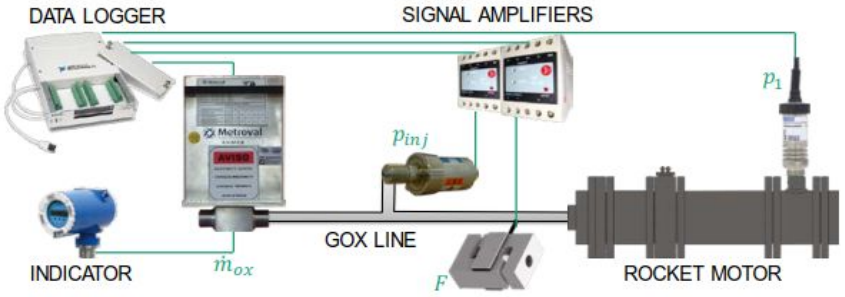

Figure 3. Parameters registered by the data acquisition board.

Although chamber adjustable maximum length is 265mm, as shown in Fig.2, maximum propellant grain length must be limited to 230 mm (as previously stated in Table 1) so that chamber pressure intake is not blocked by propellant grain. This leaves space for an after mixing chamber, which could experimentally cause unpredicted recirculation of combustion gases.

For HDPE burns, PLASTECNO grains of 66 mm in diameter and mass density of 950 kg/m^3 will be used. For HTPB burns, fuel composition grains will be HTPB as a binder pre-polymer; dioctyl-adipate (DOA) as a plasticizer and isophorone-diisocyanate (IPDI) as a cure agent, resulting in a propellant grain with density of 961 kg/m^3 . Both grains are machined to the correct size of initial port diameter (d_0) and appropriate grain length (L_P), identified through the theoretical simulation for each propellant.

4. RESULTS

4.1 Model Validation with Paraffin burn

Paraffin theoretical simulation was compared with experimental results achieved by previous work in the same test bench (Quadros 2017) and Figures 4, 5 and 6 present how main measured parameters (pressure, thrust, mass flow rate of oxidizer and regression rate) are consistent, with good accuracy, with the proposed theoretical model of this present work.

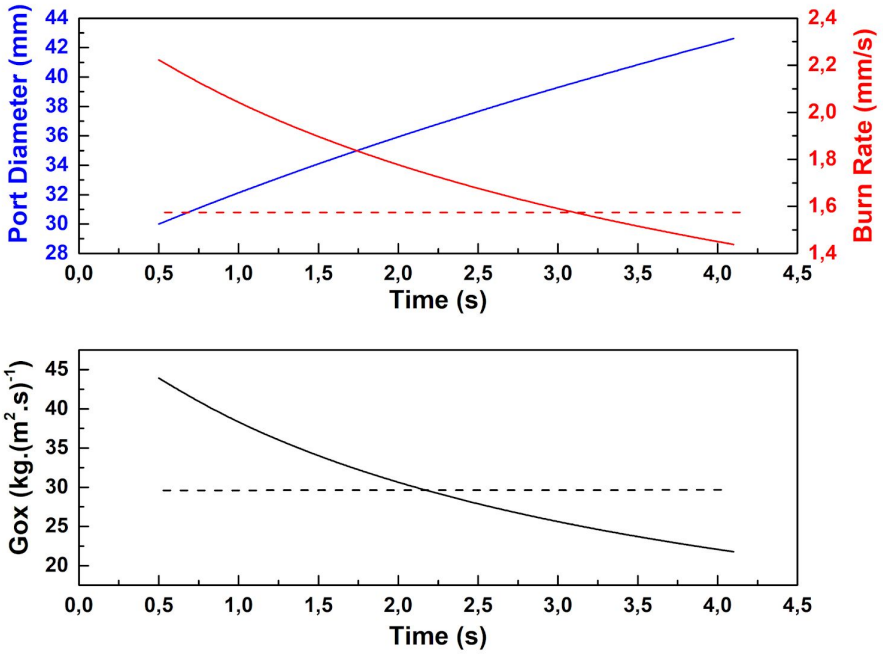

Figure 4. Propellant burn rate (upper) and G_{OX} (bottom) values from simulation (full lines) compared to experimental mean results (dashed lines). Burn starts at t = 0.5 s.

Since experimental parameters Burn rate was obtained through the measurement of grain mass before and after each burn, burn rate 1,58 mm/s and oxidant mass flux 29,7 kg/(m^2s), both represented by dashed lines in Figure 4, represent mean values (Quadros, 2017), which were be compared with simulation values by analyzing how the curves predict each parameter around mean experimental values.

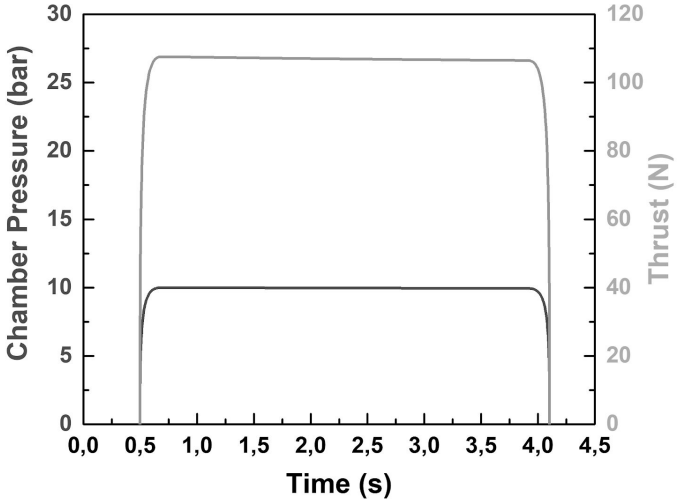

Figure 5. Chamber Pressure (p_1) and Thrust (F) simulation results for paraffin burn. Burn starts at t = 0.5 s.

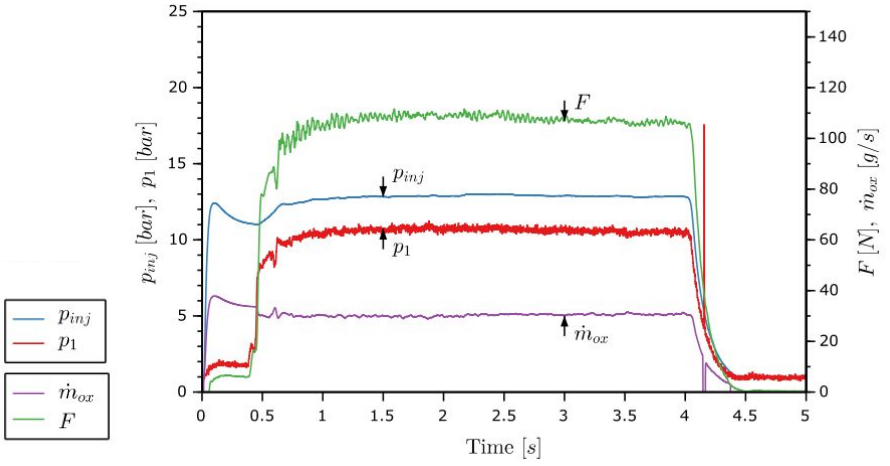

Figure 6. Chamber Pressure (p_1) and Thrust (F) experimental results for paraffin burn. Burn starts at t = 0,5 s.

4.2 Simulation Results for HDPE and HTPB

After validation of the proposed model, theoretical results (t_B, L_P, $\dot{m}_{OX}$, $p_1(t)$, $F(t)$, $r(t)$, $\dot{r}(t)$) for both HDPE and HTPB propellants are calculated as described in section 3.2 and presented in Tab. 2. Paraffin validation simulation results are included in Table 2 for comparison between fast and slow-burning fuels for hybrid rocket motors.

Table 2. Burn simulation main results for Paraffin, HDPE and HTPB burns.

Hybrid Propellant Test Bench theoretical results		Paraffin	HDPE	HTPB
[max] p_1	[bar]	10,00	6,00	3,85
[max] F	[N]	107,60	61,99	39,95
O/F (t=0)	[ ]	1,57	5,40	1,97
$\dot{m}_{OX}$	[g/s]	31,40	27,69	11,92
t_B	[s]	3,60	20,00	19,00
L_P	[mm]	107,00	230,00	226,00
r (t=0)	[mm]	15,00	6,65	10,00
r (t=t_B)	[mm]	21,23	13,54	16,49
$\dot{r}$ (t=0)	[mm/s]	2,22	0,56	0,44
$\dot{r}$ (t=t_B)	[mm/s]	1,44	0,25	0,27

Paraffin burn simulation indicates higher chamber pressure (p_1) than HDPE and HTPB burns, leading to higher thrust values, but all three cases operate below max operating chamber pressure allowed, as indicated in Tab.1. Since fuel grain length (L_P) is smaller for paraffin burn simulation, it is expected that this case operates at lower values of oxidizer to fuel ratio (O/F) in order to maintain approximate values of mass flow rate of oxidizer ($\dot{m}_{OX}$).

It is also clear in Tab. 2 that even if burning time (t_B) is 5 times shorter for Paraffin than HDPE, port diameter reduction at the end of the burn is similar when compared with HDPE burn simulation. This is due to the significant difference shown between regression rate ($\dot{r}$) for fast and slow-burning fuels for hybrid rocket motors.

Another important limitation observed in Tab.2 is that HTPB simulation values are characteristic of a low O/F burn, which is not usually studied in the literature. This limitation, though, was due to bench setup constraint, which didn't allow the use of higher values of oxidizer injection in the higher pressure oxidant line. This limitation can be clearly seen in graphics and results presented in section 4.4. Although iteration steps 1, 3 and 6 presented in Fig.1 were not achieved for HTPB, simulation, Matlab calculations were conducted either way to analyze and compare simulation parameters to experimental burn results.

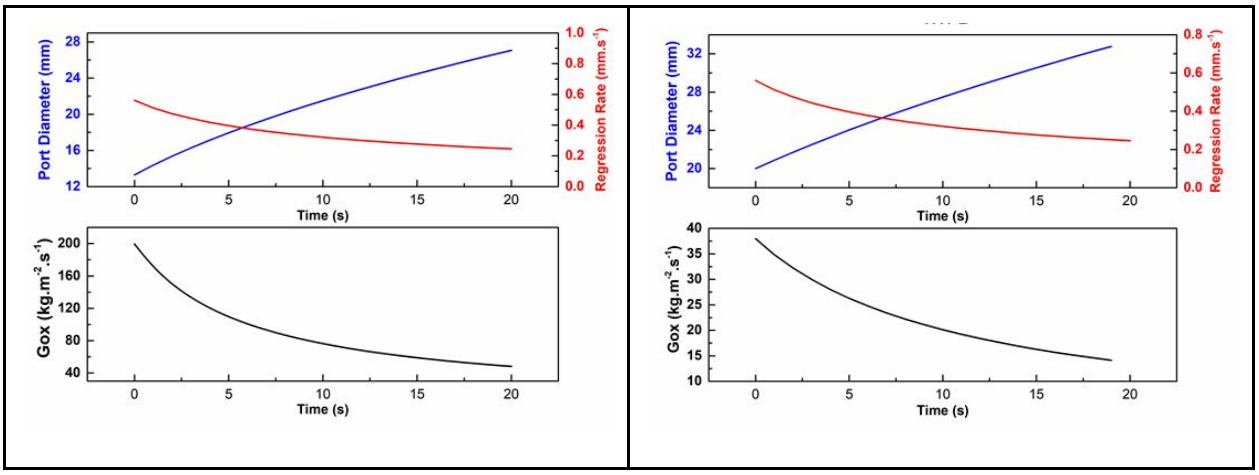

Figure 7. Simulation curves for HDPE (left) and HTPB (right) burn.

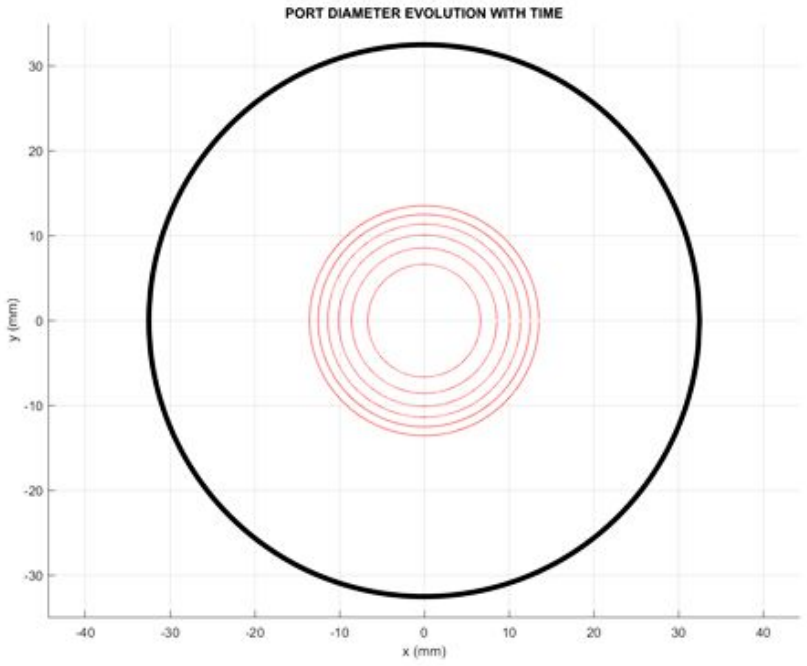

Figure 8. Representation of HDPE burn surface every 4 seconds.

Apart from these considerations for HTPB burn, oxidant mass flux (G_{OX}) values for HDPB burn were within the range established by the simulation procedure indicated in section 2.2. It can also be observed in Fig. 7 and 8 that burn rate reduces with time, so assuming constant burn rate over time in these burns could be inappropriate in case of long burn experiments.

4.3 Comparison between HDPE burn and simulation predicted parameters

Results obtained from chamber pressure transducer and thrust measurement for HDPE burn is presented in Fig.9. Both curves can be compared to estimated pressure and thrust from the theoretical model.

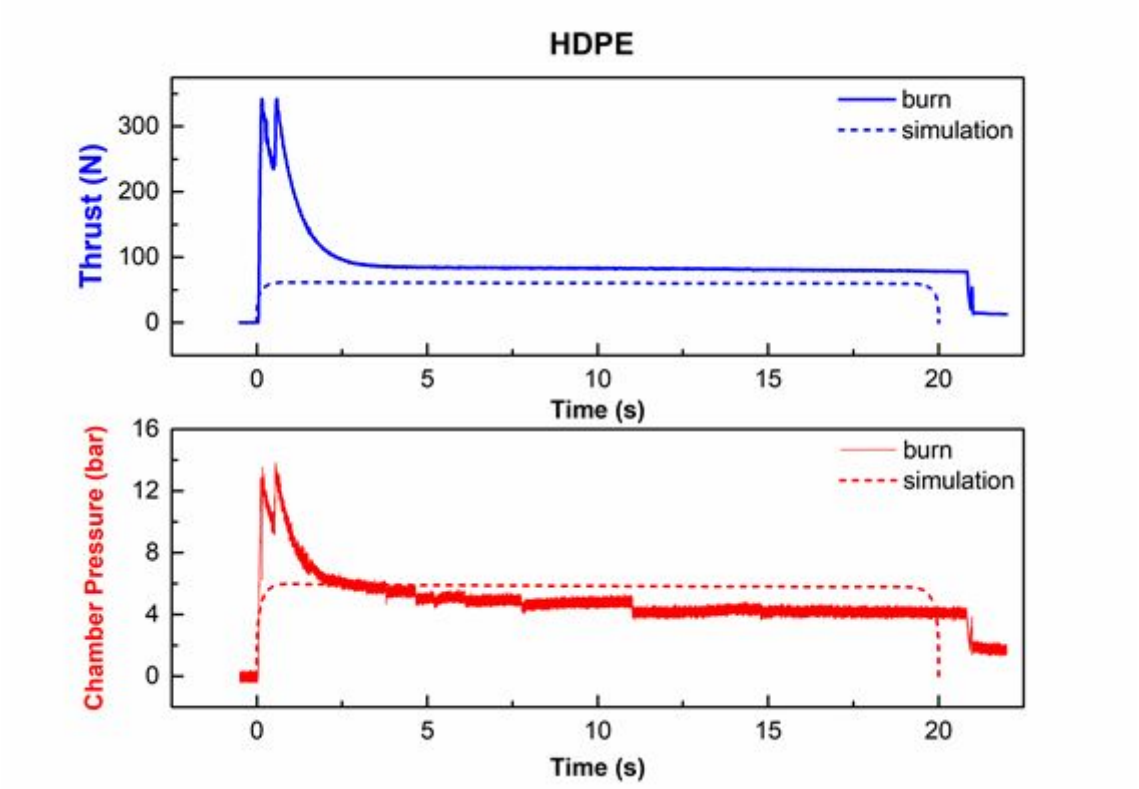

Figure 9. Thrust and chamber pressure for simulation model vs experimental measurements for HDPE burn.

Experimental burn was terminated manually, so it took more than 20 seconds of burning. As it can be seen from both thrust and pressure curves, the transient phase, which was not taken into account in the simulation model, takes approximately 3 seconds and for this short time, thrust and pressure measured were 4 times higher than predicted values. Since this transient phase was already taken into account during LCPE test bench design, it can be accepted in these HDPE burns. A comparison between Figures 6 and 9 shows that this transient phase was more controlled during paraffin burn. This is due to the setup previously used, which didn't need a low pressure injection of gaseous oxygen to start ignition of the hybrid motor, as it was stated previously in section 3.

Another factor which was not considered in the simulation model is the possible recirculation zone of combustion gases formed at the after mixing chamber, as previously stated in section 3. Since the recirculation zone is at the base of the pressure transducer, its measurements don't represent how steady the flame was after the transient phase, as it can be seen from the thrust data and also from the frames presented in Figure 10.

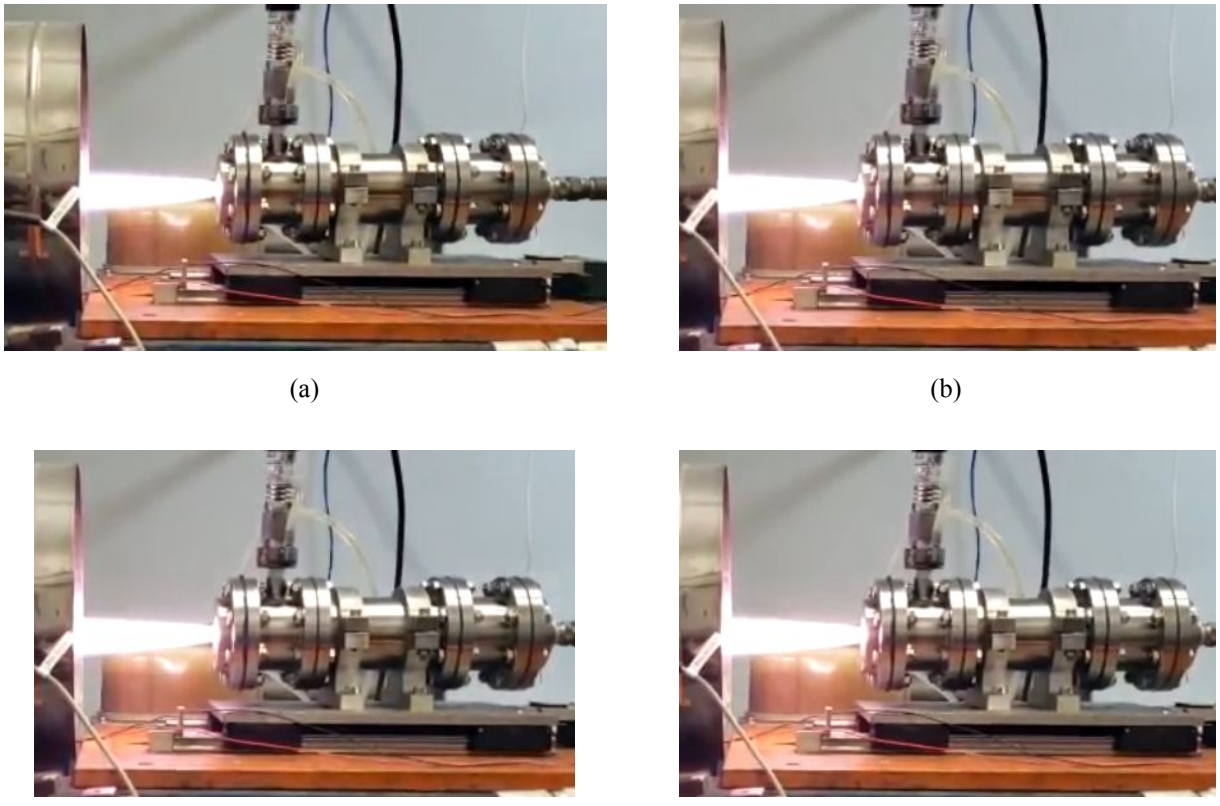

(a) (b)

(c) (d)

Figure 10. Steady flame from HDPE burn at (a) 4 seconds, (b) 8 seconds, (c) 12 seconds and (d) 16 seconds.

Another important analysis on the thrust curve shown in Figure 9 is that predicted thrust was almost 30% lower than measured values. This higher thrust can also be indirectly associated with the formation of the recirculation zone previously discussed. Since spatial distribution of the regression rate is not expected to be constant when there is occurrence of these recirculation zones (Bianchi et al., 2019), a higher regression rate at this portion of the propellant grain can contribute to the increase of measured thrust when compared to simulation expected values. This strong recirculation region could have been induced by the axial injection (Bianchi et al., 2015) and hence could be reduced by the use of a swirl injector previously used at LCPE test bench experiments. By taking these measures, measured values of thrust and pressure over time would be even more consistent with the proposed theoretical value of this work.

Although theoretical model didn't consider the effect of the above mentioned recirculation zone, inspection on the HDPE port diameter at the end of the 20 seconds burn (Fig.11) showed that while port diameter at one end of the grain changed from 13,2 mm to 14,4 mm, the other end of the grain changed from 13,2 mm to 35,4 mm.

Figure 11. Post firing HDPE grain.

Even though regression rate was not constant along grain length, an average regression rate along all the grain length could be considered to compare remaining parameters from the simulation model and experimental data. Figures 12 and 13 show these remaining data comparisons.

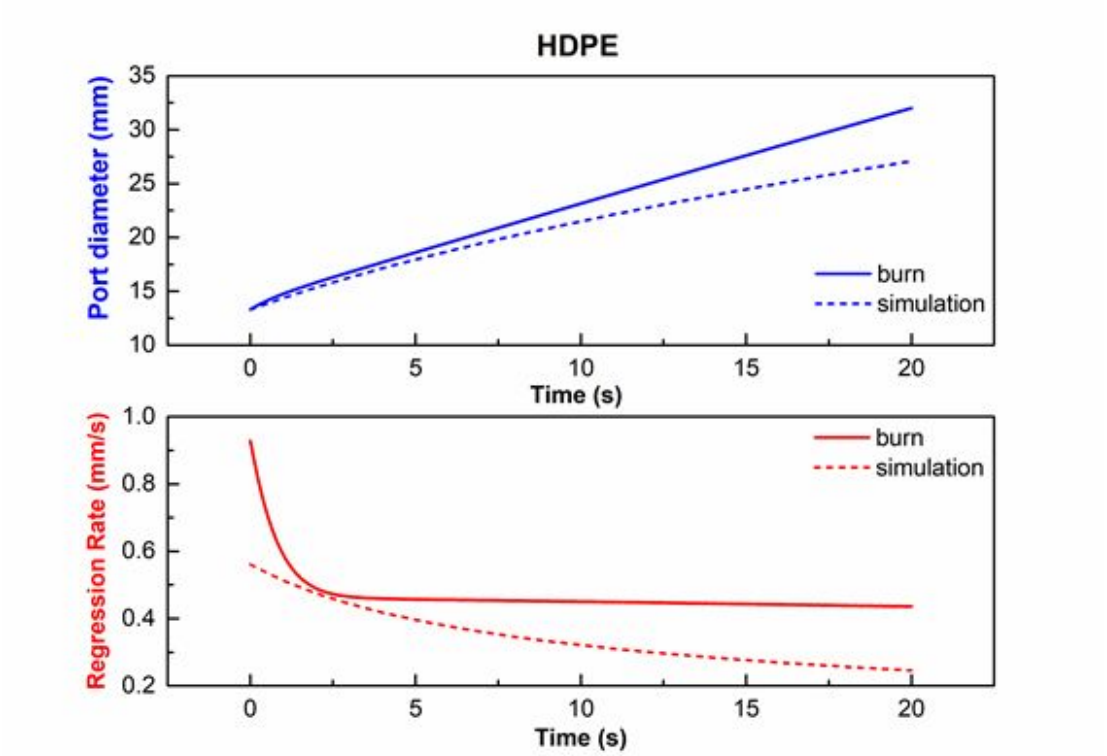

Figure 12. Port diameter and regression rate for simulation model vs calculated test parameters for HDPE burn.

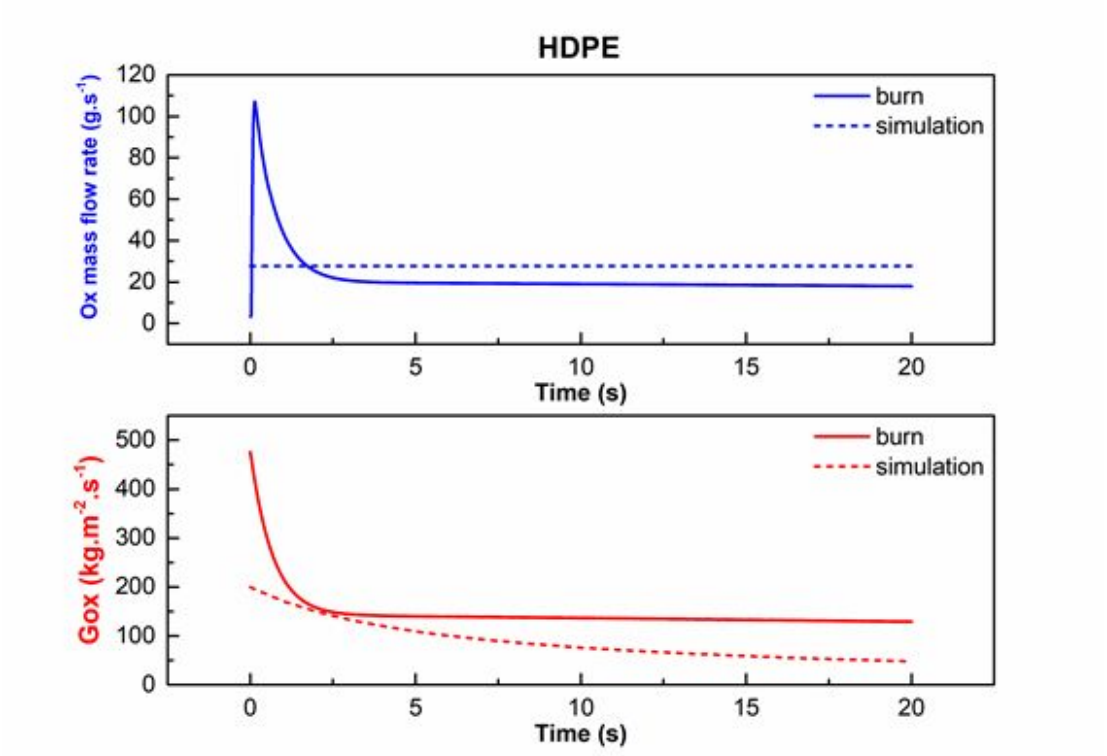

Figure 13. Gaseous oxygen mass flow rate ($\dot{m}_{OX}$) and mass flux (G_{OX}) for simulation model vs calculated test parameters for HDPE burn.

Oxidizer mass flow rate is calculated based on the measured injection pressure, considering isentropic flow through the injector. Since there is a peak initial value of oxidizer mass flow rate, the oxidizer mass flux at the first 3 seconds is significantly higher than the predicted value from the simulation model. As the experimental data reaches a more steady burn, curves showing evolution of parameters G_{OX}, port diameter and regression rate have similar behaviour when comparing theoretical model and experimental data (considering an average regression rate along all the grain length), since port diameter increases less as time passes and regression rate and oxidizer mass flux both decrease less as time passes. One important consideration is that G_{OX} is within expected range for most of the burn duration (not considering 1st second of transient phase), as stated in section 2.2, meaning coefficients "*a*" and "*n*" are appropriated to be considered in the calculation of the average regression rate using Eq.1.

4.4 Comparison between HTPB burn and simulation predicted parameters

Results obtained from chamber pressure transducer and thrust measurement for HTPB burn is presented in Fig.14. Both curves can be compared to estimated pressure and thrust from the theoretical model.

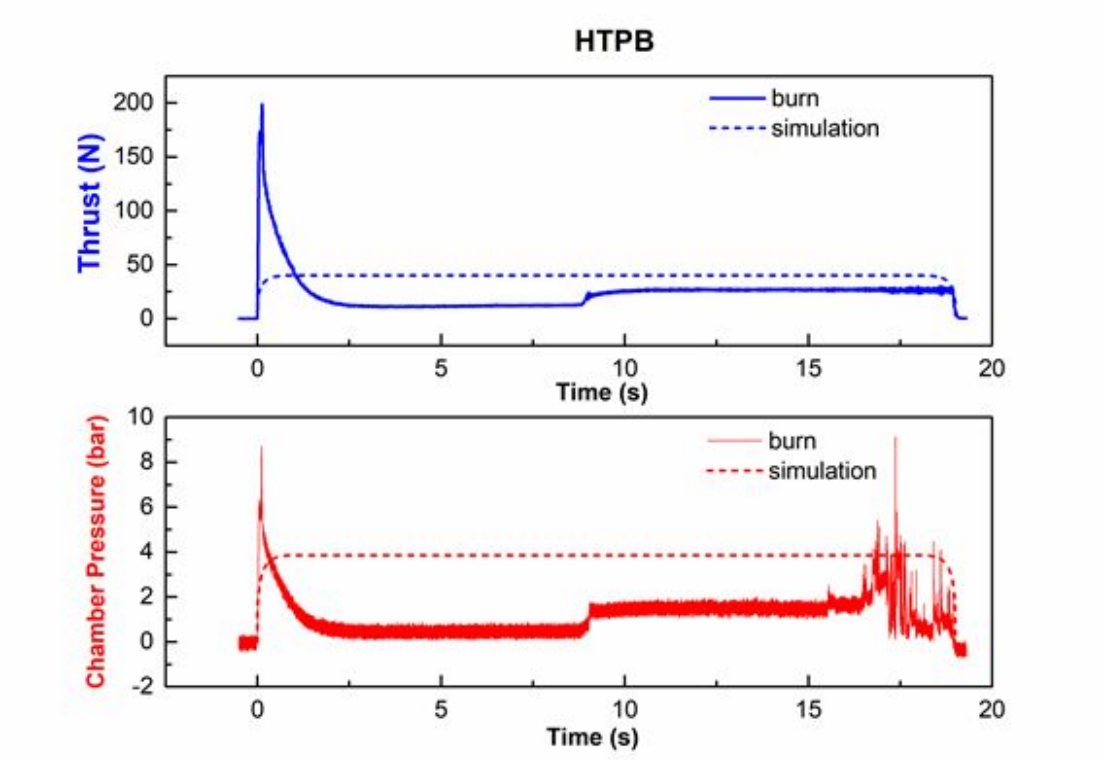

Figure 14. Thrust and chamber pressure for simulation model vs experimental measurements for HTPB burn.

Experimental burn was terminated manually, so it took little less than predicted 19 seconds of burning. Similar to HDPE burn, the transient phase, which was not taken into account in the simulation model, takes approximately 3 seconds and for this short time, thrust and pressure measured were 6 times higher than predicted values. Since this transient phase was already taken into account during LCPE test bench design, it can also be accepted in these HTPB burns.

Although theoretical model didn't consider the effect of the a recirculation zone, as indicated in section 4.3, inspection on the HTPB port diameters at the end of the 19 seconds burn showed that while port diameter at one end of the grain changed from 18,30 mm to 23,02 mm, the other end of the grain changed from 25,44 mm to 38,07 mm, confirming the occurrence of this phenomenon during the experimental burn of HTPB.

It is clear from thrust values presented in Fig.14 that, only after 9 seconds, a total ignition of the grain length occurs and, even at this stage, neither thrust nor chamber pressure values are consistent with simulation predicted values.This can be partially associated with the formation of the recirculation zone previously discussed, but it is mainly due to the experimental limitation of an extremely low oxidizer pressure line, which forced an operation at lower values of oxidizer/fuel ratio. Finally and similarly to HDPE burn, pressure values are also unstable after 16 seconds of burn due to recirculation zone effect on the location of the pressure transducer, as stated before in section 4.3.

Even though regression rate was not constant along grain length, an average regression rate along all the grain length could be considered to compare remaining parameters from the simulation model and experimental data. Figures 15 and 16 show these remaining data comparisons.

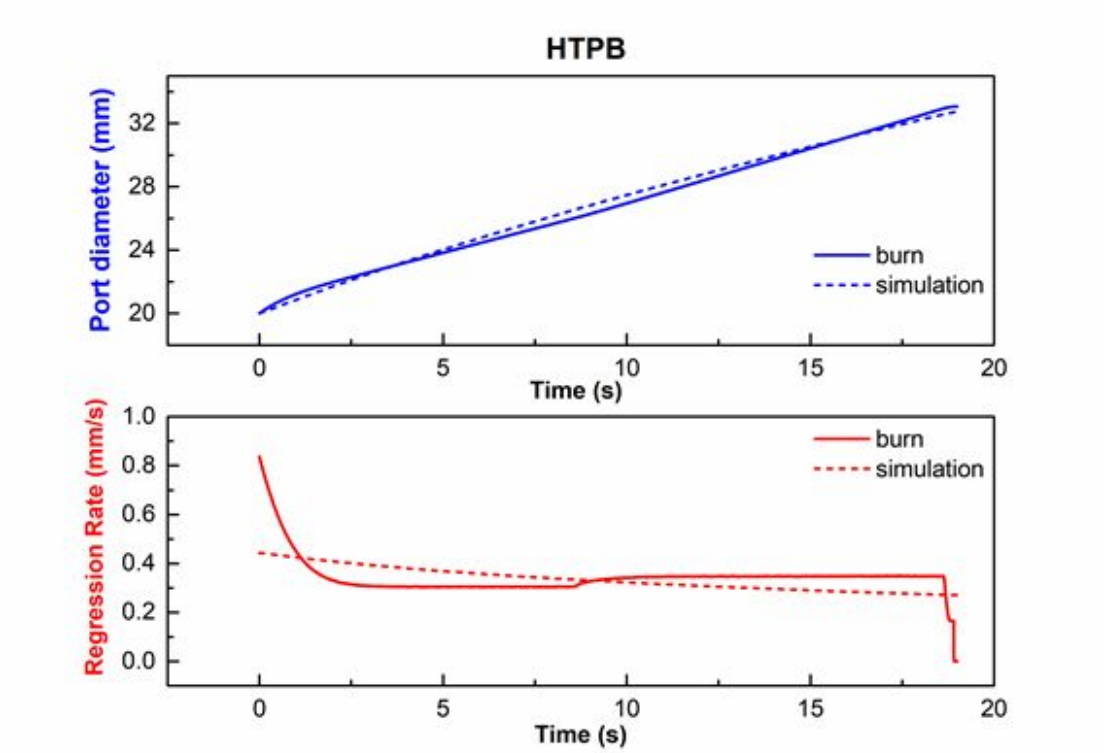

Figure 15. Port diameter and regression rate for simulation model vs calculated test parameters for HTPB burn.

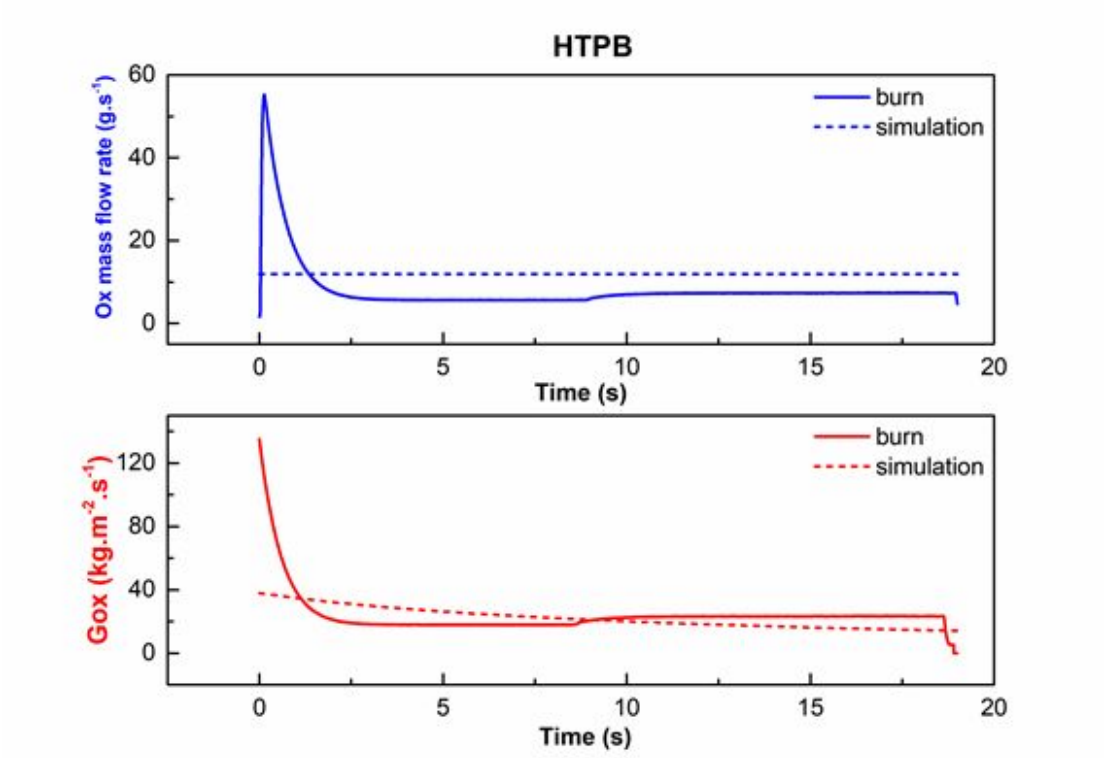

Figure 16. Gaseous oxygen mass flow rate ($\dot{m}_{OX}$) and mass flux (G_{OX}) for simulation model vs calculated test parameters for HTPB burn.

Similar to the analysis on HDPE Figures 12 and 13, there is a peak initial value of oxidizer mass flow rate and oxidizer mass flux at the first 3 seconds. After total ignition of the grain length at 9 seconds, regression rate increases and consequently, port diameter grows faster than the beginning of the burn, reaching, at the end of the burn, an equivalent port diameter similar to the one predicted by the simulation model (considering an average regression rate along all the grain length). It is important to highlight that differently from HDPE simulation, iteration steps 1, 3 and 6 presented in Fig.1 were not achieved for HTPB, simulation, meaning theoretical model could be significantly improved for this type of propellant if there was no oxidizer pressure line constraint at LCPE for this experiment..

5. CONCLUSIONS

The proposed simulation procedure presented in this work was validated by comparison to Paraffin burns previously made at LCPE test bench, showing good accuracy with experimental results, as shown in Figures 4, 5 and 6. For HDPE and HTPB comparisons, it was observed undesired events such as recirculation zone formed at the after mixing chamber and also an experimental constraint of the oxygen supply line for HTPB burns. Although pressure and thrust curves obtained from simulation results do not consider transient phase and also doesn't not consider differential variation of regression rate along the length of the grain, results obtained showed good prediction on the correct behaviour of port diameter and regression rate for HDPE burn, even if values obtained were 30% different due to these said undesired and unpredicted phenomena.

In conclusion, this work proved to be the first step in order to the definition of a simulation procedure which enables the reutilization of a pre-existing hybrid rocket test bench with any different hybrid propellant desired. In order to accomplish a final version of this simulation model, efforts are still being made in order to minimize undesired events, which could be beneficial in many ways. Given the fact that the use of these test benches represents cost reduction while enabling the possibility to study application of new fuel blends, this work can be considered of great value for future studies on hybrid propulsion at LCPE.

6. ACKNOWLEDGEMENTS

The authors would like to thank the support of the staff of the laboratories LCPE and FENG, ITA.

7. REFERENCES

BIANCHI, D.; BETTI, B.; NASUTI, F.; et al., "Simulation of gaseous oxygen/hydroxyl-terminated polybutadiene hybrid rocket flowfields and comparison with experiments", *J. Propuls. Power*, vol. 31, no. 3, pp. 919-929, 2015.

BIANCHI, D.; LECCESE, G.; NASUTI, F.; et al., "Modeling of High Density Polyethylene Regression Rate in the Simulation of Hybrid Rocket Flowfields", *Aerospace,* vol. 6, issue 8, pp.1-26,2019.

CAI, G., HAO, Z., DALIN, R., AND HUI, T., "Optimal Design of Hybrid Rocket Motor Powered Vehicle for Suborbital Flight", *Aerospace Science and Technology*, Vol. 25, No. 1, 2013a, pp. 114–124. doi:10.1016/j.ast.2011.12.014

CAI, G., ZENG, P., LI, X., TIAN, H., AND YU, N., "Scale Effect of Fuel Regression Rate in Hybrid Rocket Motor", *Aerospace Science and Technology*, Vol. 24, No. 1, 2013b, pp. 141–146. doi:10.1016/j.ast.2011.11.001

GORDON, S.; MCBRIDE, B. J. "Computer Program for Calculation of Complex Chemical Equilibrium Compositions and Applications: I. Analysis". Washington, D.C.: NASA, 1994. 61 p. (NASA RP-1311).

H. NAGATA, M. ITO, T. MAEDA et al., "Development of CAMUI hybrid rocket to create a market for small rocket experiments", *Acta Astronautica*, Vol. 59, 2006, pp. 253 -258.

KARABEYOGLU, M. A.; ALTMAN, D.; CANTWELL, B. J. **"**Combustion of Liquefying Hybrid Propellants: Part 1, General Theory", *J. Propuls. Power*, vol. 18, no. 3, pp. 610–620, 2002.

KARABEYOGLU, A.; STEVENS, J.; GEYZEL, D.; CANTWELL, B.; MICHELETTI, D. "High Performance Hybrid Upper Stage Motor", in *47th AIAA/ASME/SAE/ASEE Joint Propulsion Conference & Exhibit*, 2011, vol. 47th, no. August, pp. 1–24.

KIM, S., MOON, H., KIM, J., AND CHO, J. (2015). "Evaluation of Paraffin–Polyethylene Blends as Novel Solid Fuel for Hybrid Rockets". *Journal of Propulsion and Power, 31(6), 1750–1760.* doi:10.2514/1.b35565

MAZZETTI, A.; MEROTTO, L.; PINARELLO, G. "Paraffin-based hybrid rocket engines applications: A review and a market perspective", Reference, *Acta Astronaut*., vol. 126, pp. 286–297, 2016.

NIOKA, T., TAKAHASHI, M., AND IZUMIKAWA, M., "Gas-phase ignition of a solid fuel in a hot stagnation-point flow". *Eighteenth Symposium (International) on Combustion,* pp 741-747, 198, doi:10.1016/s0082-0784(81)80078-1

OLDE, M. S., ZANDBERGEN, B. T. C., et al., "Laser Ignition and Combustion Study of KNO3-Sorbitol based Solid Propellant". *8th European Conference For Aeronautics And Aerospace Sciences (EUCASS)*. doi: 10.13009/EUCASS2019-583

PASTRONE, D. **"**Approaches to Low Fuel Regression Rate in Hybrid Rocket Engines", *International Journal of Aerospace Engineering*, v. 2012, Article ID 649753, 2012.

QUADROS, F. D. A. "Swirl Injection of Gaseous Oxygen in a Lab-Scale Paraffin Hybrid Rocket Motor". 2017. 139 f. Dissertação (Mestrado em Engenharia Aeronáutica e Mecânica). Área de Propulsão Aeroespacial e Energia – Instituto Tecnológico de Aeronáutica, São José dos Campos.

WANG, Z.; LIN, X.; LI, F.; YU, X. "Combustion performance of a novel hybrid rocket fuel grain with a nested helical structure", *Aerosp. Sci. Technol.*, vol. 97, pp. 1–8, 2020.

8. RESPONSIBILITY NOTICE

The authors are the only responsible for the printed material included in this paper.